Published in final edited form as:

Atmos Environ (1994). 2019 ; 213: 456–462. doi:10.1016/j.atmosenv.2019.06.005.

α-Pinene-Derived Organic Coatings on Acidic Sulfate Aerosol Impacts Secondary Organic Aerosol Formation from Isoprene in a Box Model

Ryan Schmedding[1], **Mutian Ma**[1], **Yue Zhang**[1,2], **Sara Farrell**[1], **Havala O. T. Pye**[3], **Yuzhi Chen**[1], **Chi-tsan Wang**[1], **Quazi Z. Rasool**[1], **Sri H. Budisulistiorini**[4], **Andrew P. Ault**[5,6], **Jason D. Surratt**[1], and **William Vizuete**[*,1]

[1]Department of Environmental Science and Engineering, Gillings School of Public Health, University of North Carolina at Chapel Hill, Chapel Hill, North Carolina 27599 United States

[2]Aerodyne Research Inc., Billerica, Massachusetts 01821, United States

[3]Environmental Protection Agency at Research Triangle Park, Research Triangle Park, North Carolina 27711, United States

[4]Earth Observatory of Singapore, Nanyang Technological University, Singapore 639798

[5]Department of Chemistry, College of Literature, Science, and the Arts, University of Michigan, Ann Arbor, Michigan 48109, United States

[6]Department of Environmental Health Sciences, School of Public Health, University of Michigan, Ann Arbor, Michigan 48109, United States

Abstract

Fine particulate matter ($PM_{2.5}$) is known to have an adverse impact on public health and is an important climate forcer. Secondary organic aerosol (SOA) contributes up to 80% of $PM_{2.5}$ worldwide and multiphase reactions are an important pathway to form SOA. Aerosol-phase state is thought to influence the reactive uptake of gas-phase precursors to aerosol particles by altering diffusion rates within particles. Current air quality models do not include the impact of diffusion-limiting organic coatings on SOA formation. This work examines how α-pinene-derived organic coatings change the predicted formation of SOA from the acid-catalyzed multiphase reactions of isoprene epoxydiols (IEPOX). A box model, with inputs provided from field measurements taken at the Look Rock (LRK) site in Great Smokey Mountains National Park during the 2013 Southern Oxidant and Aerosol Study (SOAS), was modified to incorporate the latest laboratory-based kinetic data accounting for organic coating influences. Including an organic coating influence reduced the modeled reactive uptake when relative humidity was in the 55–80% range, with predicted IEPOX-derived SOA being reduced by up to 33%. Only sensitivity cases with a large increase in Henry's Law values of an order of magnitude or more or in particle reaction rates resulted in the large statistically significant differences form base model performance. These results suggest an organic coating layer could have an impact on IEPOX-derived SOA formation and warrant consideration in regional and global scale models.

[*]*Corresponding author:* William Vizuete.

I: INTRODUCTION

Isoprene (2-methyl-1, 3-butadiene, C_5H_8) is the most abundantly emitted biogenic volatile organic compound (BVOC) on a global basis and is known to contribute to fine particulate matter ($PM_{2.5}$) via the formation of secondary organic aerosol (SOA) (Guenther et al., 2006). SOA formation occurs when isoprene reacts with hydroxyl radicals (OH) to produce isoprene hydroxyhydroperoxides (ISOPOOH) that can further react with OH to form isomeric isoprene epoxydiols (IEPOX) (St Clair et al., 2016). IEPOX can undergo reactive uptake onto an acidified sulfate aerosol producing low-volatility products that are a significant source of SOA (Bates et al., 2014; Bondy et al., 2018b; Budisulistiorini et al., 2015; Claeys et al., 2004; Edney et al., 2005; Jacobs et al., 2014; Jason D. Surratt et al., 2006; Jesse H. Kroll et al., 2006; Krechmer et al., 2015; Liao et al., 2015; Lin et al., 2013; Lin et al., 2012; Liu et al., 2015; Nguyen et al., 2015; Paulot et al., 2009; Rattanavaraha et al., 2016; Surratt et al., 2010; Zhang et al., 2011). SOA formation from the OH-initiated oxidation of isoprene is now recognized as one of the major tropospheric sources of SOA (Carlton et al., 2010; Hallquist et al., 2009; Hu et al., 2015; Noziere et al., 2015). At certain locations within the southeastern US it has been estimated that this pathway accounts for up to 41% of the total organic mass fraction of $PM_{2.5}$ (Budisulistiorini et al., 2016; Xu et al., 2015). In this part of the US and any region with similar emission sources, a substantial organic aerosol (OA) mass fraction from isoprene contributing towards $PM_{2.5}$ requires an accurate representation of SOA formation chemistry.

Isoprene derived-SOA formation has been implemented in a regional scale air quality models (AQMs), the Community Multiscale Air Quality Model (CMAQ 5.1) and Goddard Earth Observing System (GEOS-Chem), using a heterogeneous reaction parametrization defined by a reactive uptake coefficient (γ) (Budisulistiorini et al., 2017; Pye et al., 2013). While laboratory experiments of IEPOX uptake are often performed using pure inorganic seed, one critical assumption invoked in the CMAQ model is that the aerosol with which IEPOX reacts consists of one homogeneous, internally mixed phase consisting of all organic and inorganic particulate components with no diffusion limitations. In the polluted boundary layer, it is known that acidic sulfate particles rarely exist in pure form (Hatch et al., 2011) and in the southeast US sulfate is almost always mixed with organic material at the individual particle level (Bondy et al., 2018a). Further, these particles may not be homogeneously mixed, and thus, have both diffusion limitations and reduced solubility (Craig et al., 2017; Hatch et al., 2011).

Studies have shown that both laboratory-generated and atmospheric SOA particles can be either homogenous or heterogeneous and the organic phase of heterogeneous particles can change from liquid to glassy phase state depending on the relative humidity (RH), temperature, and degree of functionalization of the compounds that these particles are comprised of (Pajunoja et al., 2013; Renbaum-Wolff et al., 2013; Rothfuss and Petters, 2017; Vaden et al., 2011; Virtanen et al., 2010; Wang et al., 2012; Zhang et al., 2015). Song et al. (2018) found that droplets containing organic and inorganic mixtures can undergo liquid-liquid phase separation when the oxygen-to-carbon (O:C) of the organic component is low (<0.56) in a low RH (<50%) environment, while no phase separation was observed

when the O:C ratio was high (>0.8). The mixed inorganic-organic aerosols may also undergo phase separation due to efflorescence, deliquescence, and/or “salting out” of the inorganic components (Ault and Axson, 2017; Freedman, 2017; O’Brien et al., 2015; Renbaum-Wolff et al., 2016; Ryder et al., 2014; Smith et al., 2013; You et al., 2012). Slade et al. (2019) showed that a diurnal cycle of phase separation and particle viscosity at a forested site impacted by transported urban air masses. Pye et al.(2018) predicted organic and inorganic constituents within accumulation mode aerosols are phase separated 70% of the time in the southeastern US during summer with potentially more frequent phase separation in urban areas and the western US. With a decrease in RH from 95% to 5%, the liquid phase of SOA can change to semi-solid or even glassy leading to phase separation (Grayson et al., 2016; Kidd et al., 2014; Renbaum-Wolff et al., 2013; Zhang et al., 2015). This phase separation, with a viscous organic shell, has the potential to hinder SOA formation, change the sensitivity of model predictions to changes in sulfate, and have potentially important implications for how efficiently BVOC-derived SOA can be produced via heterogeneous reactions (Gaston et al., 2014b; Koop et al., 2011; Shiraiwa and Seinfeld, 2012; Shiraiwa et al., 2013).

Recently laboratory data have demonstrated that pre-existing organic coatings impede the reactive uptake of IEPOX onto acidic sulfate particles. Riva et al. (2016) found that α-pinene coatings on SOA could hinder the reactive uptake of IEPOX by as much as 80% at RH levels of 50%. Gaston et al. (2014a) found that increasing the mass fraction of polyethylene glycol -derived coatings on ammonium sulfate and ammonium bisulfate aerosols reduced the γ of IEPOX under 3 different RH conditions (30, 50, and 70%). A recent study by Zhang et al., (2018), used a flow tube reactor to systematically examine the impacts of reactive uptake and found that pre-existing SOA coatings, with a coating thickness of only 10 nm, on acidic sulfate aerosol can substantially reduce the γ values for IEPOX, in some cases up to 50%.

These new results suggest that the inorganic and organic components of the aerosol particles, as well as their physical and chemical properties, jointly impact the formation, evolution, and fate of ambient SOA. Current AQMs do not include how phase separation into an organic-rich shell and inorganic-rich core may affect IEPOX uptake (a coating effect), and thus, there exists great uncertainty in our predictive ability. This work used a box model that incorporates the latest laboratory-based kinetic data and field data from the 2013 South Oxidant Aerosol Study (SOAS) to allow analysis of sensitivities to critical parameters needed to simulate the coating effects in acid-catalyzed reactive uptake of IEPOX. SOAS also provided particle-phase filter data of known isoprene SOA constituents including organosulfates and methyltetrols for use in model evaluation and parameter optimization.

II. MATERIALS AND METHODS

2.1 Reactive Uptake Algorithm

The formation of IEPOX-derived SOA is modeled in this work as a first order heterogeneous uptake reaction described elsewhere and provided in Equations S1–S7 and Table S1 (Budisulistiorini et al., 2017; Pye et al., 2013). The heterogeneous reaction is parametrized, like in CMAQ v5.1–5.2, using a γ, but assuming a core-shell morphology with an additional

coating term as shown in Equation 1 and terms are defined in the Supplementary Information (Gaston et al., 2014a; Gaston et al., 2014b).

$$\frac{1}{\gamma} = \frac{1}{\alpha} + \frac{v}{4H * R * T\sqrt{D_a * k_{particle}}} \frac{1}{\coth(q) - \frac{1}{q}} + \frac{v * l_{org} * r_p}{4 * H_{org} * R * T * D_{org} * r_{core}} \quad (1)$$

2.2 Box Model

The equations described above were implemented in a revised version of the box model used by Budisulistiorini et al. (2017) via Matlab software (version 2017a) to predict hourly average SOA concentrations, defined as the sum of IEPOX-OS and 2-methyltetrol concentrations. The amount of processing time that accounts for the atmospheric photooxidation during the day must also be assumed for this model. Using filter data Budisulistiorini et al. (2017) assumed a processing time of 6 hours which gave a reasonable simulation of the split of IEPOX-OS and 2-methyltetrol SOA found on the filters. Longer processing times overpredicted the concentration of 2-methyltetrols by a factor of 2.3 and under predicted the concentration of IEPOX-OS by a factor of 0.7 and did not reflect the total SOA mass found on the filters as well. It is not possible to robustly constrain the model processing time without air mass history given the model construction and therefore this 6 hour processing time value is used in all simulations described here. All model simulations were completed from June 1, 2013 until July 15, 2013 using SOAS 2013 field measurement at the LRK site as input based on previous work with details found in the SI. A base simulation was run as a control that reproduced the results Budisulistiorini et al. (2017) and omitted the third coating term in Equation 1.

For these simulations an accommodation coefficient (α) of 0.2 (Serway, 2009) and Henry's Law constant for the aqueous phase (H) of 3×10^7 M/atm (Budisulistiorini et al., 2017; Pye et al., 2013) were assumed to match the values used in CMAQ v5.2. The effects of adsorption of IEPOX onto the particle were assumed to be negligible due to competition with water molecules for adsorption sites (Pye et al. 2018).As shown in Table 1, the effect of RH on the solubility of IEPOX into the organic coating was assumed to be inconsequential, and a Henry's law constant for the organic coat (H_{org}) value of 2×10^5 M/atm was used as reported in literature (Gaston et al., 2014a; Gaston et al., 2014b). The thickness of the organic coat (l_{org}) is estimated to be 17 nm assuming a monodisperse aerosol distribution and calculated using the mass concentration, number concentration, and size of monoterpene-derived SOA reported during the 2013 SOAS campaign (Zhang et al. 2018; Y Zhang et al. 2015) and calculated using Equation 2.

$$l_{org} = \sqrt[3]{\frac{3}{4\pi}\frac{V}{N} + r_p^3} - r_p \quad (2)$$

The estimation of the diffusion coefficient of IEPOX in the organic coating (D_{org}) were based on two methodologies. The first relied on SOA viscosity measurements generated

from indoor flow tube studies (Shrestha et al., 2013; Zhang et al., 2015). In these studies, SOA was produced in a flow tube reactor with or without an α-pinene coating at several RH levels. The Stokes-Einstein Equation was then used to convert viscosity into diffusivity. The data provided by Zhang et al. (2015) was obtained from experiments with a RH range of 15% to 80% and is shown in Figure S1. In this study, an extrapolation of the D_{org} was used for RH < 15%. However, the D_{org} value is assumed to revert to the default value of 1×10^{-9} m^2/s used in CMAQv5.1 when RH > 80% as shown in Equation 3.

$$D_{org} = e^{6.55 * RH - 34.49} * 10^{-4} \; when \; RH < 80\% \quad (3)$$
$$D_{org} = 10^{-9} \quad when \; RH > 80\%$$

A second methodology for estimating D_{org} used a resistance model and measurements from a potential aerosol mass (PAM) reactor (Zhang et al., 2018) to derive the value of $H_{\text{org}}*D_{\text{org}}$ at various RH levels as shown in Table 1 as ap2D$_{\text{org}}$ (also shown in Figure S1). An extrapolation of the D_{org} was used for RH < 15%, while the D_{org} is assumed to revert to the value of 1×10^{-9} m^2/s when RH > 80% as shown in Equation 3. For RH from 50–80% the value of D_{org} was derived by measuring the viscosity of the coating and then using the viscosity-diffusivity relationship given by the Stokes-Einstein Equation. For RH from 15–50%, the value of $H_{org}*D_{org}$ was derived using a model fit of experimental data, and with and assumed H_{org}, the D_{o}rg relationship to RH was estimated using Equation 4.

$$D_{org} = 10^{-16.821 + \frac{5.2725}{1 + \frac{e^{74.99 * RH * 100}}{4.0633}}} * 10^{-4} \; when \; RH < 80\% \quad (4)$$

$$D_{org} = 10^{-9} \quad when \; RH > 80\%$$

III. RESULTS

The model used in this study generated 792 hours of predicted IEPOX-derived SOA that were then averaged to match the 65 3- and 11-hour filters that were collected at the LRK site. The first simulation is the “base” simulation where IEPOX SOA formation was predicted by Equation 1, but without the third term, making it identical to the implementation in Budisulistiorini et al. (2017). In the next two simulations the full Equation 1 with the coating term was implemented using parameters derived by Shrestha et al. (2013) and (Zhang et al. (2015) (ap1D$_{\text{org}}$), or from Zhang et al. (2018) (ap2D$_{\text{org}}$), as shown in Table 1. The addition of organic coatings in simulations ap1D$_{\text{org}}$ and ap2D$_{\text{org}}$ further reduced the predicted amount of IEPOX uptake and amount of SOA produced for every simulation. On average, the ap1D$_{\text{org}}$ simulation predicted a 12.7% (maximum 33.4%) reduction in total IEPOX-derived SOA when compared to predictions from the base simulation, and on average 4.73% (maximum 33.6%) reduction in case of ap2D$_{\text{org}}$. Figure 1

shows the predicted total IEPOX-derived SOA for each filter period and shows that predictions from both the $ap1D_{org}$ and $ap2D_{org}$ simulations were lower than the base simulation. Figure S2 shows the observed versus predicted SOA mass for the base, $ap1D_{org}$, and $ap2D_{org}$ simulations. The $ap1D_{org}$ simulation predictions resulted in a decrease of the slope from 1.07 in the base simulation to 0.466. However, no significant increase in values R^2 compared to the base simulation was observed. For $ap2D_{org}$, the slope was reduced to 0.866, but similarly no significant change in R^2.

The Normalized mean bias (NMB) and normalized mean error (NME), calculated by Equations 5–6, are provided in Table 2.

$$NMB = \frac{\sum_1^N (Model - Obs)}{\sum_1^N (Obs)} * 100 \quad (5)$$

$$NME = \frac{\sum_1^N |Model - Obs|}{\sum_1^N (Obs)} * 100 \quad (6)$$

where *Model* are model predictions and *Obs* are the measurement data from the LRK site.

As shown in Table 2 the predictions from the base model had a bias of −66.2% and the reductions in SOA mass in the two coating simulations further increased that negative bias. The $ap1D_{org}$ simulation decreased the NMB by 12.7% and decreased the NME marginally and $ap2D_{org}$ worsened overall model performance decreasing NMB by 4.73% and some marginal increase in NME (Table 2). Figure S3 shows the change in percentage error from the base simulation versus the RH measured at the LRK site. All changes in error occurred at RH < 85%. The figure also shows some increases in error when coating impacts are included. However, there was no statistically significant relationship between the RH and the difference in error from the Base Simulation for the simulations in the figure. All model simulations predicted the largest negative errors at the mass concentrations < 0.5 $\frac{\mu g}{m^3}$ as shown in Figure S4.

The effect of the coating term is strongly dependent on RH as the largest decreases in γ were found to occur at lower RH values. For RH > 80%, all simulations behaved like the base case. Figure 2 shows the distribution of average D_{org} values for each filter sampling period as predicted by the 792 hours generated by the model. The figure shows that most predictions occurred when the RH was between 70–95%, with only 18 filters that were predicted with an average RH of 55–60%. Above 80% RH, both $ap1D_{org}$ and $ap2D_{org}$ converged resulting in a negligible influence by coatings. For RH < 65%, $ap2D_{org}$ has a higher D_{org} than $ap1D_{org}$ by an order of magnitude. As shown in Figure S1, for RH between 65–80%, $ap2D_{org}$ exhibits a transition period where it is highly sensitive to changes in RH and the calculated D_{org} rapidly increases by 5 orders of magnitude from the values at RHs

below 65%. The inclusion of this change in D_{org} in the 65–80% RH transition period caused increase in both γ and production of SOA compared to the ap1D_{org} fit, which did not include a transition period. Figure 3 shows the resulting γ values used in these simulations and percentage reductions from the base simulation. Both ap1D_{org} and ap2D_{org} simulations showed reductions in γ for all data with RH less than 80%, with ap1D_{org} exhibiting larger reductions than ap2D_{org}.

3.1 Model Sensitivity

Uncertainty in the coating algorithms was explored via model sensitivity simulations for changes in Equation 1 to the following parameters: $k_{particle}$, H, H_{org}, D_{org}, and l_{org}. Table 1 summarizes the values for the parameters used in these simulations. The new $k_{particle}$ simulation explored the sensitivity of the inclusion of organics (Equation S7) in to the volume for the calculation of $k_{particle}$. The inclusion of a dilution effect of organics in the reacting core has the impact of lowering the particle-phase rate constant i.e. $k_{particle}$. A sensitivity run, named new $k_{particle}$, as an upper bound excluded all organics from the volume of the reacting core as shown in equation S8. The new H simulation increased H to 3×10^8 *M/atm,* which is within the reported upper range found in the literature (Riedel et al., 2015; Riedel et al., 2016). The new H_{org} simulation increased H_{org} to a value of 3×10^7 *M/atm* as an upper bound test. The thick and thin coat simulations focused on the sensitivity of SOA formation when coating thickness (Equation 2) was changed to 11.9 *nm* or 22.1 *nm*, which represents a 30% decrease or increase respectively in the estimated coating thickness by Zhang et al. (2018).

Figure 4 shows the correlation of total modeled SOA versus observations for all sensitivity simulations. As shown in Figure 4, the largest changes in predicted SOA mass occurred when H was increased. With a 10 time increase in the value of H, the new H simulation predicted 7 times increase in the slope of the fit line over the IEPOX-derived SOA predicted by ap2D_{org} and changed a 66% underprediction to a 124% overprediction as shown in Table 2 and Figure 4. The larger value for H increased γ by increasing the prediction of IEPOX's ability to partition into the aqueous phase. The increase in H_{org} in the new H_{org} simulation also produced increases in predicted SOA relative to ap2D_{org}. As shown in Table 2, these increases however resulted in no statistically significant difference in model performance of the new H_{org} resembling that of the base simulation, in terms of marginal changes in NMB and NME. The data in Figure 4 shows that modifying the coating thickness had little impact on SOA predictions. The thin coat simulation had decreased the correlation by 0.23 and the NMB by 2.84%, with marginal increase in the slope of the fit to the observed data. The thick coat decreased the correlation by 0.14 and the NMB by 6.32% from the base, with marginal reduction in the slope of the fit to the observed SOA. In the simulation that excluded the dilution by organics in $k_{particle}$ (new $k_{particle}$), the result was an increase in predicted SOA mass compared to ap2D_{org} and a slope of 1.48. Although not as much as the new H simulation, the exclusion of organics from $k_{particle}$ calculations also led to a decrease in NMB to 36.3% and NME to 77.9%. This combination of excluding organics, a H of 3.0×10^7 *M/atm*, H_{org} of 2×10^5 *M/atm*, and a D_{org} estimated from Equation 4 (Zhang et al., 2018) minimized bias and error compared to all other runs. The modification made on this simulation increased SOA mass for all conditions with or without coatings. This increase in

all predictions improved overall model performance with a statistically significant change in bias from the base simulation ($p = 0.008$) and a moderately statistically significant difference in error from the base ($p = 0.05$). The predicted increases in SOA mass from the new $k_{particle}$ simulation is shown in Figure 1 in comparison with predictions from the base simulation, $ap1D_{org}$, $ap2D_{org}$ for the time period during which the filter samples were taken.

As a sensitivity for D_{org}, an alternative formulation (Equation 7) was used that was derived from viscosity measurements taken from isoprene oxidation flow reactor experiments. This D_{org} has most recently been used in CMAQv5.2 simulations to predict isoprene-derived SOA ($isopD_{org}$) (Pye et al. 2017).

$$D_{org} = 10^{7.18 * RH - 12.7} * 10^{-4} \quad (7)$$

The $isopD_{org}$ simulation changed the D_{org} relationship as shown in Figure 2. The $isopD_{org}$ simulation predicts an exponential relationship with RH like $ap1D_{org}$, except for RH < 80% where it predicts D_{org} values that are 5 orders of magnitude higher than $ap1D_{org}$ and $ap2D_{org}$. The D_{org} values predicted by $isopD_{org}$ are large enough that the reduction in γ is negligible at any RH in the simulations, implying IEPOX uptake in CMAQ is not currently impacted by diffusivity limitations. At RH values above the cutoff, the average predicted SOA mass generated by the three different implementations converged to constant values for each filter collection period. At RH > 80%, the values of D_{org} were high enough that the resistance from the coating was insufficient to inhibit SOA formation. There was no statistical significance in the bias and error of the isopDorg simulation when compared to the base simulation.

IV: DISCUSSION

The inclusion of a coating term in the reactive uptake algorithm reduced the amount of predicted SOA mass by up to 33%. The predicted effect of the coating is most sensitive to H, causing large increases in predicted SOA mass. Preventing organic constituents from diluting the inorganic reacting volume ($k_{particle}$ calculation) also substantially increased predicted SOA mass, but not as much as increasing H. The model was least sensitive to changes in l_{org}. The model predictions also showed that the D_{org} relationship with RH is a critical parameter and large differences exist in current published models, especially when RH is less than 80%. These results highlight the importance in future models and experiments to use atmospherically-relevant SOA tracers and integrating particle viscosity measurements into the fitting parameters. It is a challenge, however, to accurately constrain the new parameters used in this model due to the fixed 6 hour chemical processing time (Budisulistiorini et al. (2017). A change in the processing time would affect model results and produce different parameter values as a best fit. Thus, these results should be viewed in terms of relative changes compared with the base simulation.

This work uses a D_{org} that was derived from α-pinene oxidation products and only represents part of the organic aerosol constituents in the real atmosphere. Other constituents including anthropogenic and other biogenic sources could have a different impact on γ.

Furthermore, the RH-dependent D_{org} functions used were derived from experimental conditions that were only limited to RH < 80%. ISORROPIA II (Fountoukis and Nenes, 2007) output was used to predict H^+ and aerosol water assuming ambient SOA forms a distinct electrolyte- rich aqueous phase and electrolyte-poor organic phase at thermodynamic equilibrium. Because of the difficulty in separating the effects of limitations in diffusivity and solubility in the coating, determining a better constrained H_{org} parameterization through laboratory experiments could lead to more scientifically sound results as well, while maintaining the same relative contributions of 2-methyltetrols and IEPOX-organosulfates. Constraining H and H_{org} would allow for the effects of model processing times to be better explored as well. Studies on constraining H, D_{org}, and H_{org} in the resistance model, and including organic interactions in $k_{particle}$, could improve model accuracy, provide a more accurate SOA formation pathway for IEPOX, and lead to more informed decisions for regional control strategies.

Supplementary Material

Refer to Web version on PubMed Central for supplementary material.

Acknowledgements:

We would like to thank Douglass Worsnop and Andrew Lambe from Aerodyne, Inc. for their help with the laboratory data used as inputs in this paper. The preparation of this paper was funded by a grant from the Texas Air Quality Research Program (AQRP) at The University of Texas at Austin through the Texas Emissions Reduction Program (TERP) and the Texas Commission on Environmental Quality (TCEQ). The findings, opinions and conclusions are the work of the author(s) and do not necessarily represent findings, opinions, or conclusions of the AQRP or the TCEQ.

References

Ault AP, Axson JL, 2017 Atmospheric Aerosol Chemistry: Spectroscopic and Microscopic Advances. Anal. Chem 89, 430–452. [PubMed: 28105816]

Bates KH, Crounse JD, St Clair JM, Bennett NB, Nguyen TB, Seinfeld JH, Stoltz BM, Wennberg PO, 2014 Gas Phase Production and Loss of Isoprene Epoxydiols. J. Phys. Chem. A 118, 1237–1246. [PubMed: 24476509]

Bondy AL, Bonanno D, Moffet RC, Wang B, Laskin A, Ault AP, 2018a Diverse Chemical Mixing States of Aerosol Particles in the Southeastern United States. Atmos. Chem. Phys. Discuss 2018, 1–37.

Bondy AL, Craig RL, Zhang Z, Gold A, Surratt JD, Ault AP, 2018b Isoprene-Derived Organosulfates: Vibrational Mode Analysis by Raman Spectroscopy, Acidity-Dependent Spectral Modes, and Observation in Individual Atmospheric Particles. J. Phys. Chem. A 122, 303–315. [PubMed: 29219314]

Budisulistiorini H, Nenes A, Carlton AG, Surratt J, McNeill VF, Pye HO, 2017 Simulating Aqueous-Phase Isoprene-Epoxydiol (IEPOX) Secondary Organic Aerosol Production During the 2013 Southern Oxidant and Aerosol Study (SOAS). Envionmental Science & Technoloy 51, 5026–5034.

Budisulistiorini SH, Baumann K, Edgerton ES, Bairai ST, Mueller S, Shaw SL, Knipping EM, Gold A, Surratt JD, 2016 Seasonal characterization of submicron aerosol chemical composition and organic aerosol sources in the southeastern United States: Atlanta, Georgia,and Look Rock, Tennessee. Atmos. Chem. Phys 16, 5171–5189.

Budisulistiorini SH, Li X, Bairai ST, Renfro J, Liu Y, Liu YJ, McKinney KA, Martin ST, McNeill VF, Pye HOT, Nenes A, Neff ME, Stone EA, Mueller S, Knote C, Shaw SL, Zhang Z, Gold A, Surratt JD, 2015 Examining the effects of anthropogenic emissions on isoprene-derived secondary organic

aerosol formation during the 2013 Southern Oxidant and Aerosol Study (SOAS) at the Look Rock, Tennessee ground site. Atmos. Chem. Phys 15, 8871–8888.

Carlton AG, Pinder RW, Bhave PV, Pouliot GA, 2010 To What Extent Can Biogenic SOA be Controlled? Environ. Sci. Technol 44, 3376–3380. [PubMed: 20387864]

Claeys M, Graham B, Vas G, Wang W, Vermeylen R, Pashynska V, Cafmeyer J, Guyon P, Andreae MO, Artaxo P, Maenhaut W, 2004 Formation of secondary organic aerosols through photooxidation of isoprene. Science 303, 1173–1176. [PubMed: 14976309]

Craig RL, Bondy AL, Ault AP, 2017 Computer-controlled Raman microspectroscopy (CC-Raman): A method for the rapid characterization of individual atmospheric aerosol particles. Aerosol Sci. Technol 51, 1099–1112.

Edney EO, Kleindienst TE, Jaoui M, Lewandowski M, Offenberg JH, Wang W, Claeys M, 2005 Formation of 2-methyl tetrols and 2-methylglyceric acid in secondary organic aerosol from laboratory irradiated isoprene/NOX/SO2/air mixtures and their detection in ambient PM2.5 samples collected in the eastern United States. Atmos. Environ 39, 5281–5289.

Fountoukis C, Nenes A, 2007 ISORROPIA II: a computationally efficient thermodynamic equilibrium model for K+-Ca2+-Mg2+-Nh(4)(+)-Na+-SO42--NO3--Cl--H2O aerosols. Atmos Chem Phys 7, 4639–4659.

Freedman MA, 2017 Phase separation in organic aerosol. Chemical Society Reviews 46, 7694–7705. [PubMed: 29134986]

Gaston CJ, Riedel TP, Zhang ZF, Gold A, Surratt JD, Thornton JA, 2014a Reactive Uptake of an Isoprene-Derived Epoxydiol to Submicron Aerosol Particles. Environ. Sci. Technol. 48, 11178–11186. [PubMed: 25207961]

Gaston CJ, Thornton JA, Ng NL, 2014b Reactive uptake of N2O5 to internally mixed inorganic and organic particles: the role of organic carbon oxidation state and inferred organic phase separations. Atmos. Chem. Phys 14, 5693–5707.

Grayson JW, Zhang Y, Mutzel A, Renbaum-Wolff L, Böge O, Kamal S, Herrmann H, Martin ST, Bertram AK, 2016 Effect of varying experimental conditions on the viscosity of α-pinene derived secondary organic material. Atmos. Chem. Phys 16, 6027–6040.

Guenther A, Karl T, Harley P, Wiedinmyer C, Palmer PI, Geron C, 2006 Estimates of global terrestrial isoprene emissions using MEGAN (Model of Emissions of Gases and Aerosols from Nature). Atmos. Chem. Phys 6, 3181–3210.

Hallquist M, Wenger JC, Baltensperger U, Rudich Y, Simpson D, Claeys M, Dommen J, Donahue NM, George C, Goldstein AH, Hamilton JF, Herrmann H, Hoffmann T, Iinuma Y, Jang M, Jenkin ME, Jimenez JL, Kiendler-Scharr A, Maenhaut W, McFiggans G, Mentel TF, Monod A, Prevot ASH, Seinfeld JH, Surratt JD, Szmigielski R, Wildt J, 2009 The formation, properties and impact of secondary organic aerosol: current and emerging issues. Atmos. Chem. Phys 9, 5155–5236.

Hatch L, Creamean J, Ault A, Surratt J, Chan M, Seinfeld J, Edgerton E, Su Y, Prather K, 2011 Measurements of Isoprene-Derived Organosulfates in Ambient Aerosols by Aerosol Time-of-Flight Mass Spectrometry - Part 1: Single Particle Atmospheric Observations in Atlanta. Environmental Science & Technology 45, 5105–5111. [PubMed: 21604734]

Hu WW, Campuzano-Jost P, Palm BB, Day DA, Ortega AM, Hayes PL, Krechmer JE, Chen Q, Kuwata M, Liu YJ, de Sa SS, McKinney K, Martin ST, Hu M, Budisulistiorini SH, Riva M, Surratt JD, St Clair JM, Isaacman-Van Wertz G, Yee LD, Goldstein AH, Carbone S, Brito J, Artaxo P, de Gouw JA, Koss A, Wisthaler A, Mikoviny T, Karl T, Kaser L, Jud W, Hansel A, Docherty KS, Alexander ML, Robinson NH, Coe H, Allan JD, Canagaratna MR, Paulot F, Jimenez JL, 2015 Characterization of a real-time tracer for isoprene epoxydiols-derived secondary organic aerosol (IEPOX-SOA) from aerosol mass spectrometer measurements. Atmos. Chem. Phys 15, 11807–11833.

Jacobs MI, Burke WJ, Elrod MJ, 2014 Kinetics of the reactions of isoprene-derived hydroxynitrates: gas phase epoxide formation and solution phase hydrolysis. Atmospheric Chemistry and Physics 14, 8933–8946.

Surratt Jason D., Murphy Shane M., Kroll Jesse H., Ng Nga L., Hildebrandt Lea, Sorooshian Armin, Szmigielski Rafal, Vermeylen Reinhilde, Maenhaut Willy, Claeys Magda, Richard C Flagan a., Seinfeld John H.*, 2006 Chemical Composition of Secondary Organic Aerosol Formed from the Photooxidation of Isoprene.

Kroll Jesse H., Ng Nga L., Murphy Shane M., Richard C Flagan a., Seinfeld JH, 2006 Secondary Organic Aerosol Formation from Isoprene Photooxidation.

Kidd C, Perraud V, Wingen LM, Finlayson-Pitts BJ, 2014 Integrating phase and composition of secondary organic aerosol from the ozonolysis of α-pinene. Proc. Natl. Acad. Sci. USA 111, 7552–7557. [PubMed: 24821796]

Koop T, Bookhold J, Shiraiwa M, Poschl U, 2011 Glass transition and phase state of organic compounds: dependency on molecular properties and implications for secondary organic aerosols in the atmosphere. Phys. Chem. Chem. Phys 13, 19238–19255. [PubMed: 21993380]

Krechmer JE, Coggon MM, Massoli P, Nguyen TB, Crounse JD, Hu W, Day DA, Tyndall GS, Henze DK, Rivera-Rios JC, Nowak JB, Kimmel JR, Mauldin RL 3rd, Stark H, Jayne JT, Sipila M, Junninen H, Clair JM, Zhang X, Feiner PA, Zhang L, Miller DO, Brune WH, Keutsch FN, Wennberg PO, Seinfeld JH, Worsnop DR, Jimenez JL, Canagaratna MR, 2015 Formation of Low Volatility Organic Compounds and Secondary Organic Aerosol from Isoprene Hydroxyhydroperoxide Low-NO Oxidation. Environ Sci Technol 49, 10330–10339. [PubMed: 26207427]

Liao J, Froyd KD, Murphy DM, Keutsch FN, Yu G, Wennberg PO, St Clair JM, Crounse JD, Wisthaler A, Mikoviny T, Jimenez JL, Campuzano-Jost P, Day DA, Hu W, Ryerson TB, Pollack IB, Peischl J, Anderson BE, Ziemba LD, Blake DR, Meinardi S, Diskin G, 2015 Airborne measurements of organosulfates over the continental U.S. J Geophys Res Atmos 120, 2990–3005. [PubMed: 26702368]

Lin YH, Zhang HF, Pye HOT, Zhang ZF, Marth WJ, Park S, Arashiro M, Cui TQ, Budisulistiorini H, Sexton KG, Vizuete W, Xie Y, Luecken DJ, Piletic IR, Edney EO, Bartolotti LJ, Gold A, Surratt JD, 2013 Epoxide as a precursor to secondary organic aerosol formation from isoprene photooxidation in the presence of nitrogen oxides. Proc. Natl. Acad. Sci. U. S. A 110, 6718–6723. [PubMed: 23553832]

Lin YH, Zhang Z, Docherty KS, Zhang H, Budisulistiorini SH, Rubitschun CL, Shaw SL, Knipping EM, Edgerton ES, Kleindienst TE, Gold A, Surratt JD, 2012 Isoprene epoxydiols as precursors to secondary organic aerosol formation: acid-catalyzed reactive uptake studies with authentic compounds. Environ. Sci. Technol 46, 250–258. [PubMed: 22103348]

Liu Y, Kuwata M, Strick BF, Geiger FM, Thomson RJ, McKinney KA, Martin ST, 2015 Uptake of epoxydiol isomers accounts for half of the particle-phase material produced from isoprene photooxidation via the HO2 pathway. Environ Sci Technol 49, 250–258. [PubMed: 25375412]

Nguyen TB, Crounse JD, Teng AP, St Clair JM, Paulot F, Wolfe GM, Wennberg PO, 2015 Rapid deposition of oxidized biogenic compounds to a temperate forest. Proc Natl Acad Sci U S A 112, E392–401. [PubMed: 25605913]

Noziere B, Kaberer M, Claeys M, Allan J, D'Anna B, Decesari S, Finessi E, Glasius M, Grgic I, Hamilton JF, Hoffmann T, Iinuma Y, Jaoui M, Kahno A, Kampf CJ, Kourtchev I, Maenhaut W, Marsden N, Saarikoski S, Schnelle-Kreis J, Surratt JD, Szidat S, Szmigielski R, Wisthaler A, 2015 The Molecular Identification of Organic Compounds in the Atmosphere: State of the Art and Challenges. Chem. Rev 115, 3919–3983. [PubMed: 25647604]

O'Brien RE, Wang B, Kelly ST, Lundt N, You Y, Bertram AK, Leone SR, Laskin A, Gilles MK, 2015 Liquid–Liquid Phase Separation in Aerosol Particles: Imaging at the Nanometer Scale. Environ. Sci. Technol 49, 4995–5002. [PubMed: 25850933]

Pajunoja A, Malila J, Hao L, Joutsensaari J, Lehtinen KEJ, Virtanen A, 2013 Estimating the viscosity range of SOA particles based on their coalescence time. Aerosol Sci. Technol 48, i–iv.

Paulot F, Crounse JD, Kjaergaard HG, Kurten A, St Clair JM, Seinfeld JH, Wennberg PO, 2009 Unexpected Epoxide Formation in the Gas-Phase Photooxidation of Isoprene. Science 325, 730–733. [PubMed: 19661425]

Pye HOT, Pinder RW, Piletic IR, Xie Y, Capps SL, Lin Y-H, Surratt JD, Zhang Z, Gold A, Luecken DJ, Hutzell WT, Jaoui M, Offenberg JH, Kleindienst TE, Lewandowski M, Edney EO, 2013 Epoxide Pathways Improve Model Predictions of Isoprene Markers and Reveal Key Role of Acidity in Aerosol Formation. Environ. Sci. Technol 47, 11056–11064. [PubMed: 24024583]

Rattanavaraha W, Chu K, Budisulistiorini SH, Riva M, Lin Y-H, Edgerton ES, Baumann K, Shaw SL, Guo H, King L, Weber RJ, Neff ME, Stone EA, Offenberg JH, Zhang Z, Gold A, Surratt JD, 2016 Assessing the impact of anthropogenic pollution on isoprene-derived secondary organic aerosol

formation in PM2.5 collected from the Birmingham, Alabama, ground site during the 2013 Southern Oxidant and Aerosol Study. Atmospheric Chemistry and Physics 16, 4897–4914.

Renbaum-Wolff L, Grayson JW, Bateman AP, Kuwata M, Sellier M, Murray BJ, Shilling JE, Martin ST, Bertram AK, 2013 Viscosity of α-pinene secondary organic material and implications for particle growth and reactivity. Proc. Natl. Acad. Sci. USA 110, 8014–8019. [PubMed: 23620520]

Renbaum-Wolff L, Song M, Marcolli C, Zhang Y, Liu PF, Grayson JW, Geiger FM, Martin ST, Bertram AK, 2016 Observations and implications of liquid–liquid phase separation at high relative humidities in secondary organic material produced by α-pinene ozonolysis without inorganic salts. Atmos. Chem. Phys 16, 7969–7979.

Riedel TP, Lin YH, Budisulistiorini H, Gaston CJ, Thornton JA, Zhang ZF, Vizuete W, Gold A, Surrattt JD, 2015 Heterogeneous Reactions of Isoprene-Derived Epoxides: Reaction Probabilities and Molar Secondary Organic Aerosol Yield Estimates. Env. Sci. Tech. Lett 2, 38–42.

Riedel TP, Zhang Z, chu K, Thornton J, Vizuete W, Gold A, surratt j.d., 2016 Constraining Condensed-Phase Formation Kinetics of Secondary Organic Aerosol Components from Isoprene Epoxydiols. Atmos Chem Phys 16, 1245–1254.

Riva M, Bell DM, Hansen A-MK, Drozd GT, Zhang Z, Gold A, Imre D, Surratt JD, Glasius M, Zelenyuk A, 2016 Effect of Organic Coatings, Humidity and Aerosol Acidity on Multiphase Chemistry of Isoprene Epoxydiols. Environ. Sci. Technol 50, 5580–5588. [PubMed: 27176464]

Rothfuss NE, Petters MD, 2017 Characterization of the temperature and humidity-dependent phase diagram of amorphous nanoscale organic aerosols. Phys. Chem. Chem. Phys 19, 6532–6545. [PubMed: 28197614]

Ryder OS, Ault AP, Cahill JF, Guasco TL, Riedel TP, Cuadra-Rodriguez LA, Gaston CJ, Fitzgerald E, Lee C, Prather KA, Bertram TH, 2014 On the Role of Particle Inorganic Mixing State in the Reactive Uptake of N_2O_5 to Ambient Aerosol Particles. Environ. Sci. Technol 48, 1618–1627. [PubMed: 24387143]

Serway R.A.a.F.J.S.a.V.C., 2009 College physics.

Shiraiwa M, Seinfeld JH, 2012 Equilibration timescale of atmospheric secondary organic aerosol partitioning. Geophys. Res. Lett 39, L24801.

Shiraiwa M, Zuend A, Bertram AK, Seinfeld JH, 2013 Gas-particle partitioning of atmospheric aerosols: interplay of physical state, non-ideal mixing and morphology. Phys. Chem. Chem. Phys 15, 11441–11453. [PubMed: 23748935]

Shrestha M, Zhang Y, Ebben CJ, Martin ST, Geiger FM, 2013 Vibrational sum frequency generation spectroscopy of secondary organic material produced by condensational growth from alpha-pinene ozonolysis. J Phys Chem A 117, 8427–8436. [PubMed: 23876044]

Slade JH, Ault AP, Bui AT, Ditto JC, Lei Z, Bondy AL, Olson NE, Cook RD, Desrochers SJ, Harvey RM, Erickson MH, Wallace HW, Alvarez SL, Flynn JH, Boor BE, Petrucci GA, Gentner DR, Griffin RJ, Shepson PB, 2019 Bouncier Particles at Night: Biogenic Secondary Organic Aerosol Chemistry and Sulfate Drive Diel Variations in the Aerosol Phase in a Mixed Forest. Environ. Sci. Technol

Smith ML, You Y, Kuwata M, Bertram AK, Martin ST, 2013 Phase Transitions and Phase Miscibility of Mixed Particles of Ammonium Sulfate, Toluene-Derived Secondary Organic Material, and Water. J. Phys. Chem. A 117, 8895–8906. [PubMed: 23931697]

St Clair JM, Rivera-Rios JC, Crounse JD, Knap HC, Bates KH, Teng AP, Jorgensen S, Kjaergaard HG, Keutsch FN, Wennberg PO, 2016 Kinetics and Products of the Reaction of the First-Generation Isoprene Hydroxy Hydroperoxide (ISOPOOH) with OH. J Phys Chem A 120, 1441–1451. [PubMed: 26327174]

Surratt JD, Chan AW, Eddingsaas NC, Chan M, Loza CL, Kwan AJ, Hersey SP, Flagan RC, Wennberg PO, Seinfeld JH, 2010 Reactive intermediates revealed in secondary organic aerosol formation from isoprene. Proc. Natl. Acad. Sci. U. S. A 107, 6640–6645. [PubMed: 20080572]

Vaden TD, Imre D, Beránek J, Shrivastava M, Zelenyuk A, 2011 Evaporation kinetics and phase of laboratory and ambient secondary organic aerosol. Proc. Natl. Acad. Sci. USA 108, 2190–2195. [PubMed: 21262848]

Virtanen A, Joutsensaari J, Koop T, Kannosto J, Yli-Pirila P, Leskinen J, Makela JM, Holopainen JK, Poschl U, Kulmala M, Worsnop DR, Laaksonen A, 2010 An amorphous solid state of biogenic secondary organic aerosol particles. Nature 467, 824–827. [PubMed: 20944744]

Wang B, Lambe AT, Massoli P, Onasch TB, Davidovits P, Worsnop DR, Knopf DA, 2012 The deposition ice nucleation and immersion freezing potential of amorphous secondary organic aerosol: Pathways for ice and mixed-phase cloud formation. J. Geophys. Res. (Atmos.) 117, 209–220.

Xu L, Guo H, Boyd CM, Klein M, Bougiatioti A, Cerully KM, Hite JR, Isaacman-VanWertz G, Kreisberg NM, Knote C, Olson K, Koss A, Goldstein AH, Hering SV, de Gouw J, Baumann K, Lee S-H, Nenes A, Weber RJ, Ng NL, 2015 Effects of anthropogenic emissions on aerosol formation from isoprene and monoterpenes in the southeastern United States. Proc. Natl. Acad. Sci. U. S. A 112, 37–42. [PubMed: 25535345]

You Y, Renbaum-Wolff L, Carreras-Sospedra M, Hanna SJ, Hiranuma N, Kamal S, Smith ML, Zhang X, Weber RJ, Shilling JE, Dabdub D, Martin ST, Bertram AK, 2012 Images reveal that atmospheric particles can undergo liquid–liquid phase separations. Proc. Natl. Acad. Sci. USA 109, 13188–13193. [PubMed: 22847443]

Zhang H, Surratt JD, Lin YH, Bapat J, Kamens RM, 2011 Effect of relative humidity on SOA formation from isoprene/NO photooxidation: enhancement of 2-methylglyceric acid and its corresponding oligoesters under dry conditions. Atmos Chem Phys 11, 6411–6424.

Zhang Y, Chen Y, Lambe AT, Olson NE, Lei Z, Craig RL, Zhang Z, Gold A, Onasch TB, Jayne JT, Worsnop DR, Gaston CJ, Thornton JA, Vizuete W, Ault AP, Surratt JD, 2018 Effect of the Aerosol-Phase State on Secondary Organic Aerosol Formation from the Reactive Uptake of Isoprene-Derived Epoxydiols (IEPOX). Env. Sci. Tech. Lett 5, 167–174.

Zhang Y, Sanchez MS, Douet C, Wang Y, Bateman AP, Gong Z, Kuwata M, Renbaum-Wolff L, Sato BB, Liu PF, Bertram AK, Geiger FM, Martin ST, 2015 Changing shapes and implied viscosities of suspended submicron particles. Atmos. Chem. Phys 15, 7819–7829.

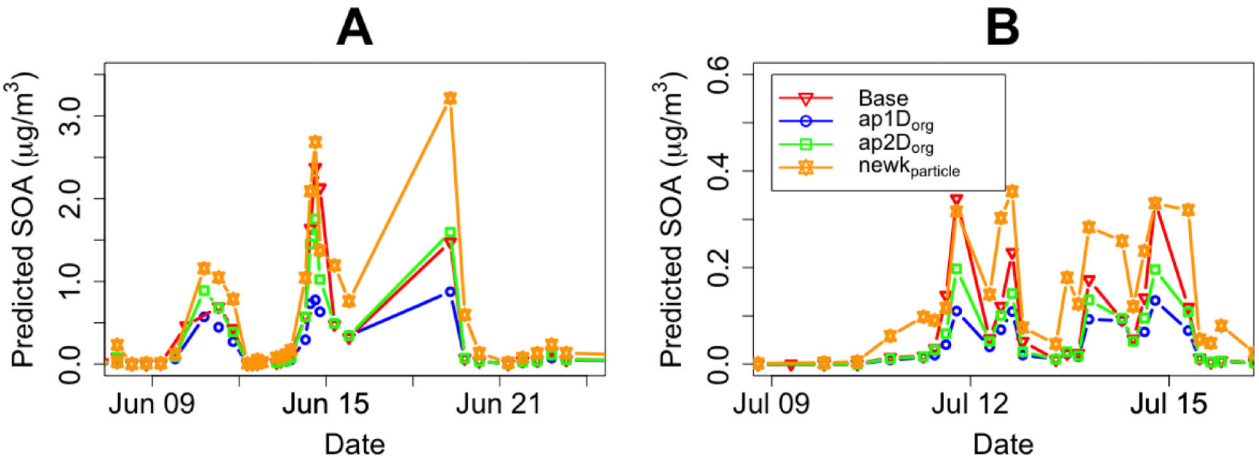

Figure 1.

Time series of total predicted IEPOX-derived SOA mass concentration from the box-model at the Look Rock site from A: June 8 to June 24, 2013 and B: July 9 to July 16, 2013 for the following simulations: base (red triangle), $ap1D_{org}$ (blue circle), $ap2D_{org}$ (green square), and New $k_{particle}$ (orange star).

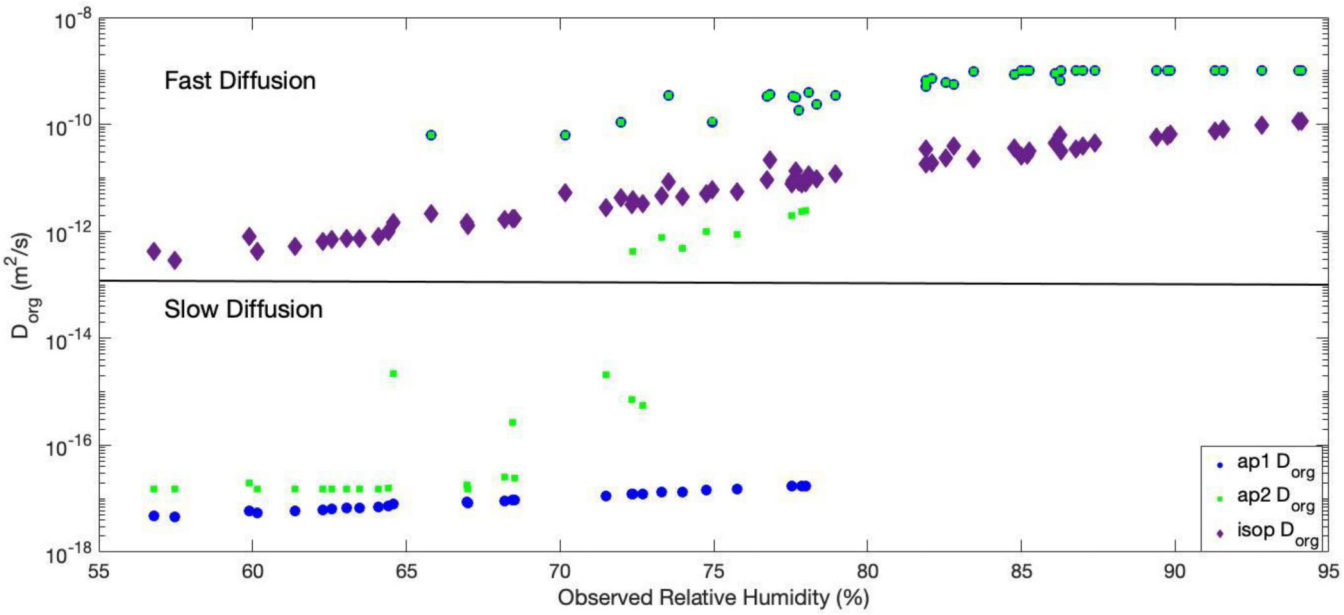

Figure 2.

D_{org} values as a function of measured RH at the Look Rock site for the ap1D_{org} (blue circle), ap2D_{org} (green square) and isopD_{org} (purple diamond) simulation, Model simulations are summarized in table 1.

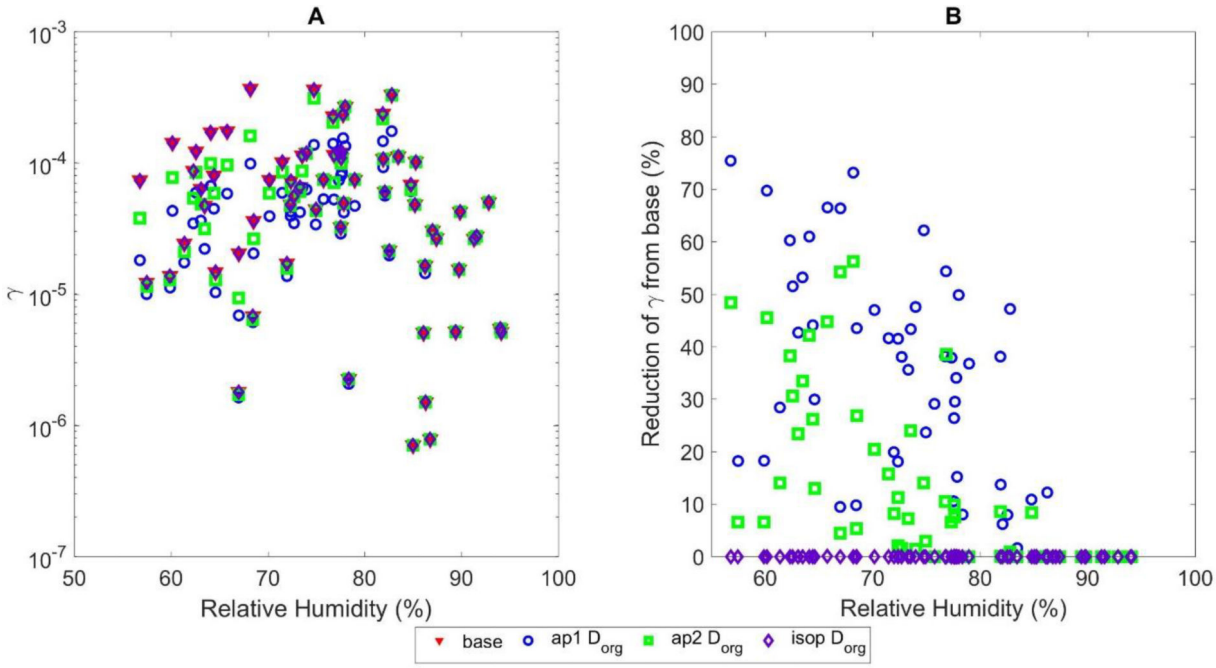

Figure 3.

(A) Predicted value of γ and (B) percent reduction in γ for the original base simulation (red triangle, subplot A only), $ap1D_{org}$ (blue circle), $ap2D_{org}$ (green square), and $isopD_{org}$ (purple diamond) simulations as a function of average relative humidity for each filter sample.

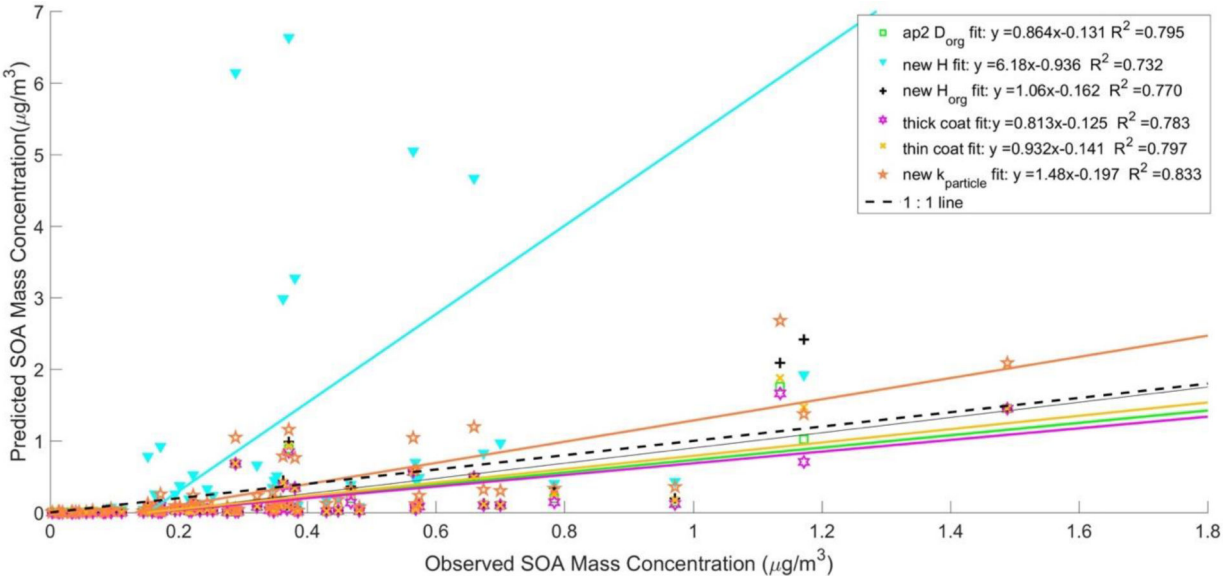

Figure 4.

Observed SOA mass vs model predicted mass for all SOA generated for the following simulations: ap2D_{org} (green square), newH (cyan triangle), newH_{org} (black plus), thick coat (magenta hexagram), thin coat (gold x), and new $k_{particle}$ (orange star).

Table 1.

Summary of parameters used in all 0-D model simulation simulations. H is the effective Henry's law constant for IEPOX partitioning onto inorganic aerosol, H_{org} is the effective Henry's law constant for IEPOX partitioning onto organic coating, RH is relative humidity, D_{org} is the IEPOX gas diffusion coefficient through organic coating, L_{org} is the thickness of coating layer. RH cutoff is the RH above which D_{org} reverts to a baseline value of 10^{-9} m^2/s. The rightmost column indicates whether the organics diluted the concentration of inorganic constituents that was used to calculate $k_{particle}$

Simulation	H (M/atm)	H_{org} (M/atm)	D_{org} (m^2/s) (RH<Cutoff)	D_{org} (m^2/s) (RH>Cutoff)	L_{org} (m)	$k_{particle}$ includes organics
Base	$3.00*10^7$	NA	NA	NA	NA	Yes
ap1D_{org}	$3.00*10^7$	$2*10^5$	$e^{6.55*RH-34.488)}*10^{-4}$	$1*10^{-9}$	$1.7*10^{-8}$	Yes
ap2D_{org}	$3.00*10^7$	$2*10^5$	$10^{(-16.821+ 5.2725/(1+e^(74.99*RH*100)/4.0633))*}$ 10^{-4}	$1*10^{-9}$	$1.7*10^{-8}$	Yes
isopD_{org}	$3.00*10^7$	$2*10^5$	$10^{(7.18*RH - 12.7)}*10^{-4}$	$1*10^{-9}$	$1.7*10^{-8}$	Yes
new $k_{particle}$	$3.00*10^7$	$2*10^5$	$10^{(-16.821+ 5.2725/(1+e^(74.99*RH*100)/4.0633))}*10^{-4}$	$1*10^{-9}$	$1.7*10^{-8}$	No
newH	$3.00*10^8$	$2*10^5$	$10^{(-16.821+ 5.2725/(1+e^(74.99*RH*100)/4.0633))}*10^{-4}$	$1*10^{-9}$	$1.7*10^{-8}$	Yes
newH_{org}	$3.00*10^7$	$3*10^8$	$10^{(-16.821+ 5.2725/(1+e^(74.99*RH*100)/4.0633))}*10^{-4}$	$1*10^{-9}$	$1.7*10^{-8}$	Yes
thin coat	$3.00*10^7$	$2*10^5$	$10^{(-16.821+ 5.2725/(1+e^(74.99*RH*100)/4.0633))}*10^{-4}$	$1*10^{-9}$	$1.19*10^{-8}$	Yes
thick coat	$3.00*10^7$	$2*10^5$	$10^{(-16.821+ 5.2725/(1+e^(74.99*RH*100)/4.0633))}*10^{-4}$	$1*10^{-9}$	$2.21*10^{-8}$	Yes

Table 2.

The normalized mean bias (NMB) and normalized mean error (NME) for total predicted IEPOX-derived SOA when compared with filter-based molecular measurements collected at the LRK site. The difference when compared with the base simulation is shown in parentheses and simulation parameters are summarized in Table 1.

Simulation	Normalized Mean Bias (Difference from base)	Normalized Mean Error (Difference from Base)
base	−66.2	83.4
ap1Dorg	−78.9 (−12.7)	83.3 (−0.10)
ap2Dorg	−70.9 (−4.73)	83.5 (0.07)
isopDorg	−68.0 (−1.84)	83.0 (−0.43)
New kparticle	−36.3 (29.9)	77.9 (−5.5)
New H	124 (190)	211 (128)
New Horg	−66.2 (−0.01)	83.4 (0.04)
thin coat	−69.0 (−2.84)	83.0 (−0.43)
thick coat	−72.5 (−6.32)	84.5 (1.07)